Separation Dynamics of Strap-On Boosters

Rajeev Lochan and V. Adimurthy
Vikram Sarabhai Space Centre, Trivandrum 695022, India
and
K. Kumar
Indian Institute of Technology, Kanpur 208016, India

The dynamics associated with the jettisoning of a number of strap-ons from the parent launch vehicle is investigated. Three different models for the separation mechanisms are considered. Included in the analysis are forces due to the jettisoning mechanism along with the thrust on the core and the residual thrust on the strap-ons. Aerodynamic forces are, however, not considered. Geometry of collision in the multibody system is analyzed and three different criteria for detection of collisions are developed. The methodology is illustrated using two typical examples. The attitude motion of the controlled ongoing stage has been indirectly accounted for. Finally, a simple representation of the separation system is employed to construct a no-collision domain in the design parameter space.

Nomenclature

b^j = body coordinates of the nozzle throat
F^j = resultant external force on the jth body
I_i^j = principal moments of inertia associated with body j about X_i^j axis; $i = 1, 2, 3$
M^j = resultant external moment on the jth body
m^j = mass of the jth body
s^j = number of side thrusters or springs
T^j = atmospheric thrust on body j
η^j = thrust misalignment/cant angle
η_p^j, ψ_p^j = angles defining the orientation of the thrust with respect to body j, similar to η^j and ψ^j
ψ^j = angle between the plane of misalignment and X_2^j axis

Subscript

$(\ )_p$ = ( ) for the pth thruster or spring

Superscript

$(\ )^j$ = ( ) for the jth body

Introduction

STRAP-ONS have been extensively used for boosting payload capabilities of launch vehicles. Jettisoning mechanisms are employed to provide for separation between the ongoing stage, called the core, and the spent strap-ons. Spring-based systems achieve this separation by commanding release of energy of the precompressed springs. Although the

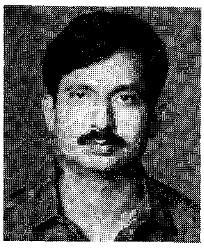

Rajeev Lochan graduated with a degree in Mechanical Engineering from BIT Sindri (Bihar), India, in 1973 and received his Master's in Aeronautical Engineering from the Indian Institute of Technology (IIT) Kanpur in 1976. He participated in the development of a trisonic wind tunnel at IIT Kanpur before joining Vikram Sarabhai Space Centre (VSSC), Trivandrum, in 1977. Since then, he has been engaged in research in diverse aspects of flight mechanics of launch vehicles. Dynamics of separating bodies, deployment dynamics, boost phase guidance, and onboard algorithms for position and attitude determination are some of the areas where he has made contributions. Currently, he is pursuing his Doctorate in Aerospace Engineering at IIT Kanpur in addition to his present responsibilities in the Aerodynamics Division of VSSC.

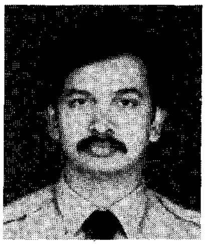

V. Adimurthy is Head of the Aerodynamics Division at Vikram Sarabhai Space Centre. Born in 1946 in Rajahmundry, India, he was educated at Andhra University, Waltair, and later at the Indian Institute of Technology Kanpur, where he received his Ph.D. in 1973. He was a Research Fellow of the Alexander von Humboldt Foundation during 1979–1980 at Stuttgart University, Germany. His contributions are in the areas of aerodynamics, flight dynamics, and trajectory optimization of aerospace vehicles.

Krishna Kumar was born in India on November 19, 1946. He received a B.S. from the University of Allahabad, India, in 1964, a B. Tech degree in Mechanical Engineering from IIT Kharagpur, India, in 1968, and a Ph.D. for work in satellite attitude dynamics and control from the University of British Columbia, Canada, in 1972. He is presently a Professor in the Department of Aerospace Engineering at the Indian Institute of Technology, Kanpur, India. His current research interests include dynamics and control of aerospace vehicles, static deformation of cables, optimization, and filtering.

Received June 7, 1990; revision received Jan. 19, 1991; accepted for publication Jan. 22, 1991.

amount of the energy that can be packed is rather limited, these systems are simple and reliable. On the other hand, if the strap-ons are massive and require large energy for separation, side thrusters may have to be employed. A judicious jettisoning system design not only ensures collision-free separation but also limits the resulting disturbances on the core to a minimum. This paper analyzes the dynamics involved in separation of strap-ons from the launch vehicle.

The general dynamics of separating bodies has received the attention of several investigators. Dwork[1] and Wilke[2] provide valuable insight into disturbances caused by separation mechanisms in a spinning setup. Longren[3] has analyzed spin-stabilized rockets with guide shoes and rails constraining the lateral motion. Waterfall[4] has investigated multispring systems for separation of spinning and nonspinning bodies. Subramanyam[5] has developed a general model for spring-assisted stage separation. Chubb[6] has constructed collision boundaries between two separating stages. Through analysis of the separation of apogee motor from payload, Biswas[7] has indicated the possibility of an increase in lifetime by nonseparation. Lochan et al.[8,9] have examined a multistep separation where a set of passenger payloads are separated from one another. However, the specific problem of separation of strap-ons from the launch vehicle appears to have received little attention in the open literature.

The dynamics of strap-on separation differs significantly from that of the other separating bodies. Unlike the general rocket-stage separation, the separation of strap-ons is accompanied by a lateral velocity component. Furthermore, the analysis of this problem requires that the thrust on the separated body also be accounted for. The analysis is further complicated by the presence of aerodynamic forces, which, however, are not considered in the present investigation.

Although a number of countries have used strap-on technology for years, no related investigations appear to have been reported in the open literature. In view of the proposed strap-on designs of the Indian Augmented Satellite Launch Vehicle (ASLV) and Polar Satellite Launch Vehicle (PSLV), Prahlad,[10] Sundaramurthy et al.,[11] and Biswas[12] have investigated several related aspects. This paper represents a systematic attempt to analyze the problem of strap-on stage separation. The various steps involved in this investigation are the following: 1) formulation and solution of the equations of motion in order to generate position and attitude history of the various bodies involved and their relative motion, 2) examination of the resulting information for establishing the cleanliness (i.e., collision-free separation) or otherwise of the separation process, and 3) analysis of the attitude motion of the core.

Formulation

Because the problem is rather involved, several simplifying assumptions are made. The separating bodies are taken to be rigid and without any dynamic imbalance. Their masses, moments of inertia, and the center of mass locations within the bodies are considered to be time invariant. Furthermore, the atmospheric corrections to thrust or residual thrust are assumed to be independent of time. These assumptions are not particularly restrictive in view of a rather short duration of the separation process (typically around 1 s).

The core, the ongoing stage, is usually controlled, whereas the strap-ons after separation are not. The dynamics of the core, therefore, needs to be treated differently from that of the strap-ons. Ideally, a complete knowledge of the control system of the core is a prerequisite to the simulation of the separation dynamics. In the proposed scheme, however, a need for simulation of the attitude control dynamics of the core has been done away with altogether. Instead, we determine its permissible deviation from the assumed ideal behavior as a design specification to be prescribed for the core control system. This approach is found to be quite useful as it leads to decoupling of the dynamics of separation from that of the core control system, thus enabling a high degree of simplification.

Let us now begin the formulation by first defining the various system parameters. Let n denote the number of bodies including the core. Let the superscript $j = 1$ represent the core while $j = 2, 3, \ldots, n$ be reserved for the $(n-1)$ strap-ons. Let t denote time as measured from the instant of separation initiation. Let the following coordinate systems be used for convenience of representation and interpretation:

1) Local core inertial frame $X_{C_1}\,X_{C_2}\,X_{C_3}$ (C frame) with origin frozen at the center of mass at $t = 0$ and taking the axis X_{C_1} along the longitudinal axis, X_{C_2} along the pitch axis, and X_{C_3} so chosen as to complete the right-handed triad. This frame is assumed to move with uniform system velocity taken at $t = 0$. Since, at this instant, the core and the strap-ons have the same orientation and velocity with reference to this C frame, the initial conditions of velocity and orientation for all of the bodies reduce to zero. The velocity of the core (and all other bodies), however, may evolve with time under the influence of external forces.

2) Local strap-on inertial frame $X^j_{S_1}\,X^j_{S_2}\,X^j_{S_3}$ (S^j frame) for the jth strap-on, with origin at its own center of mass at $t = 0$ taking $X^j_{S_1}$ parallel to X_{C_1}, $X^j_{S_2}$ along the radial direction and selecting $X^j_{S_3}$ so as to complete the right-handed triad as before.

3) Body frame $X^j_1\,X^j_2\,X^j_3$ (B^j frame) for the jth body such that the frames B^j and S^j are identical at $t = 0$.

The body frames are introduced to facilitate Eulerian description of angular motion. These noninertial frames are obtained from the inertial S^j frame (C^1 frame) by three successive rotations in the following sequence: 1) a rotation θ^j_3 about the $X^j_{S_3}$ axis ($X^1_{C_3}$ axis) leading to intermediate frame (X'_1, X'_2, X'_3), 2) a rotation θ^j_2 about the X'_2 axis leading to another intermediate frame (X''_1, X''_2, X''_3), and, finally, 3) a rotation θ^j_1 about the X''_1 axis leading to the body frame $X^j_1\,X^j_2\,X^j_3$.

At $t = 0$, the origin of the S^j frame is referred to the C frame in terms of the radial distance r^j_{S0}, the angular distance ϕ^j_{S0} and the longitudinal location h^j_{S0}. These parameters at some general time t are referred to as r^j_S, ϕ^j_S, h^j_S, respectively. The corresponding changes in the position of the jth body are denoted by Δr^j_s, $\Delta\phi^j_s$, and Δh^j_s, whereas the Cartesian coordinates of the origin of the S^j frame with respect to the C frame at some general time t are represented by U^j. Kinematic relations between the Eulerian rates $\dot\theta^j_1$, $\dot\theta^j_2$, $\dot\theta^j_3$ and components of the angular velocity of the jth body denoted by ω^j_1, ω^j_2, ω^j_3 in its respective body frame may be developed easily. Here, dots represent derivatives with respect to time. The components of the velocity of the body j with respect to the C frame and expressed in the B^j frame as v^j_1, v^j_2, v^j_3 are related to the rates of Cartesian coordinates through the transformation matrix $[B^j]$ relating B^j to the S^j frame.

Equations of Motion

The equations of translational and rotational motion for the bodies can be expressed as follows:

$$\mathring{v}^j_i - \epsilon_{ikl} v^j_k \omega^j_l = F^j_i / m^j; \qquad i = 1, 2, 3 \tag{1}$$

$$I^j_i \mathring{\omega}^j_i - \epsilon_{ikl} I^j_k \omega^j_k \omega^j_l = M^j_i; \qquad i = 1, 2, 3 \tag{2}$$

However, in view of the ideal control assumption of the core, Eq. (2) is not required for the core ($j = 1$) and it is instead replaced by the following a priori description of the angular motion:

$$\omega^1_i = \Omega_i(t) \tag{3a}$$

$$\theta^1_i = \Theta_i(t) \tag{3b}$$

External forces and moments are a consequence of gravitational pull, aerodynamic effects, thrust, residual thrust, and forces introduced by separation mechanisms. Since our interest is confined to relative motion over rather short periods of interval, the gravitational forces would have no effect and, hence, have been left out.

Next, we obtain the forces and moments due to the engine and tailoff thrusts. The resulting expression for forces F_t and moments M_t may be written as

$$F_t^j = T^j \begin{Bmatrix} \cos\eta^j \\ \sin\eta^j \quad \cos\psi^j \\ \sin\eta^j \quad \sin\psi^j \end{Bmatrix} \tag{4}$$

$$M_{t_i}^j = \epsilon_{ikl} b_k^j F_{t_l}^j \tag{5}$$

The modeling of the separation mechanism has to be rather specific to the application under consideration. Three models covering a variety of applications are considered here.

Model 1: Black Box Model

This model avoids a direct consideration of the forces and moments generated by the actual mechanism responsible for the separation. Instead, it is accounted for in terms of the changes in the state. If the separation process takes time t_1 for completion, we can write

$$\theta_i^j(t_1) = \theta_{i0}^j + \Delta\theta_i^j; \qquad j = 1,2,\ldots,n \tag{6a}$$

$$x_i^j(t_1) = x_{i0}^j + \Delta x_i^j; \qquad j = 1,2,\ldots,n \tag{6b}$$

Although this model appears rather simple, it is quite useful in deducing appropriate design parameter limits on separation mechanisms.

Model 2: Spring Assisted Separation

Here, we consider a mechanism in which the jth strap-on is jettisoned using s^j number of prestressed springs that connect it with the core (Fig. 1). Let the coordinates of the attachment points for the pth spring connecting the jth body be denoted by $e_{p_i}^j$ for the core and $f_{p_i}^j$ for the strap-ons ($p = 1, 2, \ldots s^j$) in their respective body frames.

At any instant, the location of the attachment point associated with the body j for the pth spring in the C frame is given by

$$\alpha_p^j = [S^j]^T\{[B^j]^T f_p^j + x_S^j\} + U^j; \qquad j \neq 1 \tag{7}$$

while the corresponding coordinates for the attachment point for the same spring on the core in the C frame are

$$\beta_p^j = [B^1]^T e_p^j + x_C^1 \tag{8}$$

The length of the pth spring at some instant is then given by

$$q_p^j = \|\alpha_{p_i}^j - \beta_{p_i}^j\|; \qquad j \neq 1 \tag{9}$$

and the corresponding unit vector $\hat{\nu}_p^j$ has the components

$$\hat{\nu}_{p_i}^j = (\alpha_{p_i}^j - \beta_{p_i}^j)/q_p^j; \qquad j \neq 1 \tag{10}$$

Let δ_p^j be the instantaneous deflection, Q_p^j the initial separation of the attachment points, and ρ_p^j the corresponding initial compression of the pth spring. Then,

$$Q_p^j = q_p^j|_{t=0}; \qquad j \neq 1 \tag{11a}$$

$$\delta_p^j = \rho_p^j - (q_p^j - Q_p^j); \qquad j \neq 1 \tag{11b}$$

The magnitude of the separating force S_p^j at t can be represented as

$$\begin{aligned} S_p^j &= P(\delta_p^j) \qquad &\text{if} \quad \delta_p^j > 0 \text{ and } j \neq 1 \\ &= 0 \qquad &\text{if} \quad \delta_p^j \leq 0 \text{ and } j \neq 1 \end{aligned} \tag{12}$$

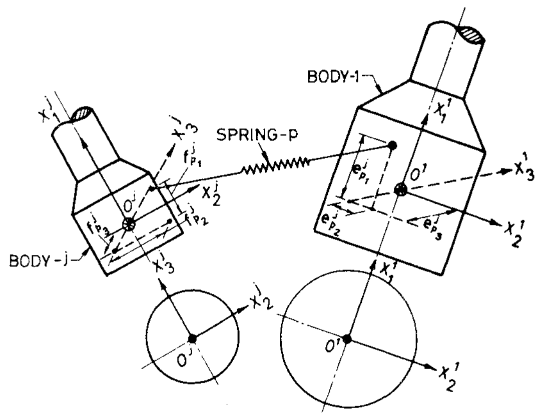

Fig. 1 Typical model of spring assisted separation system.

where P stands for a function relating the spring deflection to the separating force. It is not unusual to have nonlinear springs for this kind of application. This relationship could be implemented in polynomial form or as a table-look-up.

The body forces F_s^j and moments M_s^j on the jth body due to springs can now be written as

$$F_s^j = \sum_{p=1}^{s^j} S_p^j [B^j][S^j]\hat{\nu}_p^j; \qquad j \neq 1 \tag{13a}$$

$$M_{S_i}^j = \sum_{p=1}^{s^j} \epsilon_{ikl} f_{p_k}^j (S_p^j [B^j][S^j]\hat{\nu}_{p_l}^j); \qquad j \neq 1 \tag{13b}$$

while the corresponding net force and moment on the core due to the entire ejection mechanism take the form

$$F_s^1 = -\sum_{j=2}^{n} \sum_{p=1}^{s^j} S_p^j [B^1]\hat{\nu}_p^j; \qquad j \neq 1 \tag{14a}$$

$$M_{S_i}^1 = -\sum_{j=2}^{n} \sum_{p=1}^{s^j} \epsilon_{ikl} e_{p_k}^j (S_p^j [B^1]\hat{\nu}_{p_l}^j); \qquad j \neq 1 \tag{14b}$$

Since the attitude history of the core is prescribed a priori, one need not evaluate the expression for moment on the core due to the ejection mechanism. This moment, however, is the disturbance on the core caused by the jettisoning mechanism and may be useful for the attitude control analysis of the core.

Model 3: Side Thruster Assisted Separation

Under certain conditions, more energy for separation may be needed than can be provided by springs. This requirement can be adequately met by the use of side thrusters.

The expressions for separation forces obtained in a manner as those for engine thrust can be written as follows.

For strap-ons ($j \neq 1$):

$$F_s^j = \sum_{p=1}^{s^j} T_p^j \begin{bmatrix} \cos\eta_p^j \\ \sin\eta_p^j \quad \cos\psi_p^j \\ \sin\eta_p^j \quad \sin\psi_p^j \end{bmatrix} \tag{15}$$

For core ($j = 1$):

$$F_{s_i}^1 = M_{s_i}^1 = 0$$

The resultant external forces F^j and moments M^j on the jth body are now simply given as

$$F_i^j = F_{t_i}^j + F_{s_i}^j + F_{\alpha_i}^j; \qquad i = 1, 2, 3; j = 1, 2, \ldots, n \tag{16a}$$

$$M_i^j = M_{t_i}^j + M_{s_i}^j + M_{\alpha_i}^j; \qquad i = 1, 2, 3; j = 1, 2, \ldots, n \tag{16b}$$

Aerodynamic forces F_α and moments M_α are rather complex to model mainly because of 1) the complex interference flow field, 2) the large angles of incidence involved, and 3) the complicated body geometry. Extensive wind-tunnel testing is, therefore, normally undertaken to develop reasonable aerodynamic models for specific configurations. The aerodynamic forces and moments although important and retained in the previous expressions have not been included in the following analysis.

Evidently, it is not possible to obtain a closed-form solution for the resulting complex nonlinear nonautonomous set of differential equations governing the translational and rotational motion of the bodies involved in the separation process. For this, a general purpose software called TOSS was developed and used to study the motion numerically. All of the initial conditions required for solving the system equations are zero except ω_i^j, which is the same as the system body angular rates at $t = 0$. This follows by virtue of the specific choice of the reference systems adopted and the geometry of the strapped-on vehicle. It may also be noted that the initial orientation of the system does not affect the separation process since the orientation of the C frame does not enter into the formulation.

Geometry of Collision

Three methods, each with its own merits and demerits, are proposed for detection of collision (or absence of it). These methods utilize the time history of position and orientation generated earlier. Their relative usefulness depends on specific applications.

Method 1: No-Collision Zone

This simple scheme may be automated or used conveniently with graphics. The construction of the no-collision zone, however, is restricted to simple situations. In the most general case, the criterion for no collision between the jth body and the kth body during separation may be stated symbolically by the inequality

$$g(x_{s_i}^j,\ x_{s_i}^k,\ \theta_i^j,\ \theta_i^k) \leq 0; \qquad i = 1, 2, 3 \tag{17}$$

where the absence of derivative terms may be noted.

For illustration purposes, we take up a simple but practical case with basic cylindrical geometry for all of the bodies. In addition, the following simplifying assumptions are made.

1) Protrusions on the body, if any, are insignificant; although, in many cases, it may be possible to handle even these by assuming somewhat larger effective body diameters so as to adequately cover the protrusions.

2) The core has an infinite length, which would lead to a conservative estimate of a collision-free region actually larger than the one obtained here with this assumption.

3) The angular rotation θ_2^j for the strap-ons causing their ends to move away from their radial planes (formed by their longitudinal axes and that of the core) would reduce the possibility of collision. However, for developing a simple but conservative criterion, this out-of-plane rotation has been ignored.

A simple analysis based on relative geometry leads to the following criterion for collision-free separation:

$$D/2 + [(d^j/2)^2 + (l^j)^2]^{1/2} \sin[\theta_3^j + \arctan(d^j/2l^j)] - x_{C_2}^j < 0 \cdots \tag{18}$$

where $l^j = l_1^j$ for $\theta_3^j < 0$ and $l^j = l_2^j$ for $\theta_3^j > 0$ (Fig. 2). The results giving the boundary of the no-collision zone for a typical system with parameters as in Table 1 are presented in Fig. 2.

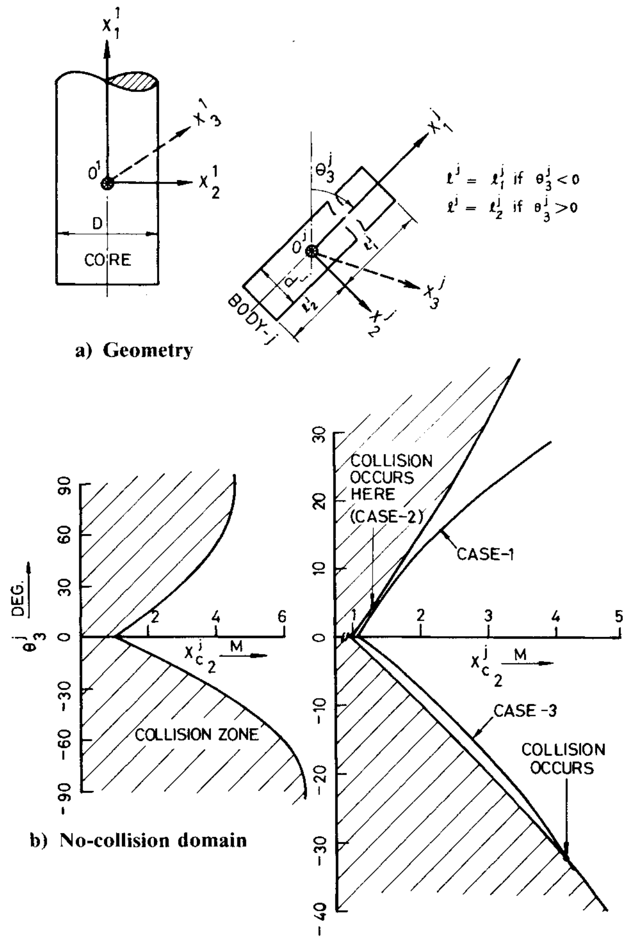

a) Geometry

b) No-collision domain

c) Enlarged view of no-collision domain

Fig. 2 No-collision zone.

Method 2: Pair of Tips

Although method 1 provides the overall information concerning the parametric limits ensuring collision-free separation, further details may be needed about certain critical parts such as protrusions, cable connections, or attachments connecting the bodies through explosive bolts. Evidently, in such applications, method 1 is not suitable and an alternate method proposed here would be more appropriate. It is based on the use of certain critical points as just indicated. We would refer to it as the pair-of-tips method. The assumption that the core is an infinite cylinder is also relaxed.

Table 1 Parameter values for the illustrative examples

System: Configuration A with side thrusters	
Mass of core	20,000 kg
Mass of each strap-on	2000 kg
Mass moment of inertia of each strap-on	500, 25,000, 25,000 kgm^2
Core thrust (constant, corrected for atmospheric pressure)	400 kN
Strap-on tailoff thrust (constant, corrected for atmospheric pressure)	35 kN
Strap-on thrust location	4 m below center of mass
Strap-on cant angle	10 deg
$D = 1$ m; $d^2 = 1$ m; $l_1^2 = 4$ m; $l_2^2 = 6$ m	
Example 1	
Number of side thrusters for each strap-on	2
Location of top thruster $b_{1,1}^2$	1.5 m
Location of bottom thruster $b_{1,2}^2$	−3.5 m
Constant thrust for top thruster (after correction)	4 kN
Constant thrust for bottom thruster (after correction)	
Case 1	5 kN
Case 2	4.5 kN
Case 3	15 kN
Example 2	
Strap-on tailoff thrust	0, 10, 20, 30 kN

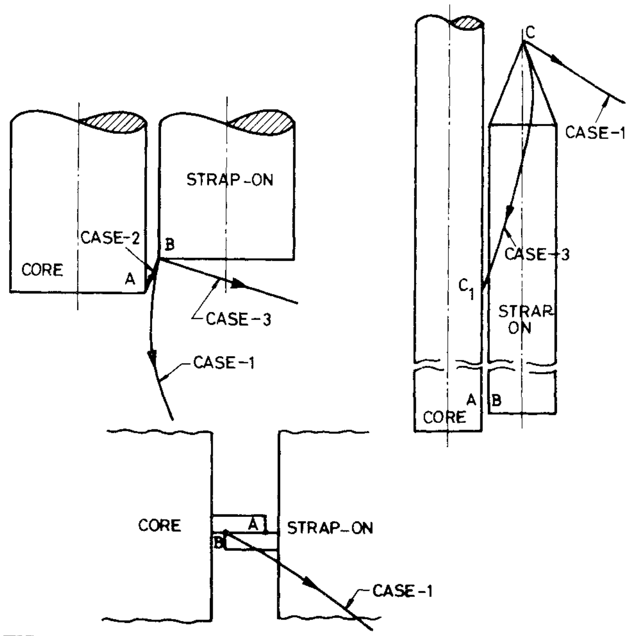

Fig. 3 Relative motion of pair of tips.

Here, the appropriate critical points or tips are first identified on each of the strap-ons along with their counterparts on the core. For each such pair of critical points, we study the motion of one with respect to the other. The expressions obtained for the components of the position vector of the second tip (associated with strap-on j) with respect to the first one (on the core) can be expressed in C frame as

$$W_C^j = [S^j]^T\{[B^j]^T\xi^j + x_s^j\} + U^j - \{[B^1]^T\xi^1 + x_C^1\} \tag{19}$$

where ξ_i^j refers to the tip coordinates associated with the jth body.

Projection of this vector on a suitable plane is now examined for investigating collisions. The plane initially containing the two longitudinal axes is chosen for the investigation. The vector components in that plane are computed by a simple transformation. For illustration, three cases are considered (Table 1). In the first one, there is no collision as the path of tip B relative to tip A indicates, whereas in the second case these collide (Fig. 3). However, in case 3, even though this locus shows an absence of collision, actually the nose of the strap-on, i.e., tip C, does hit the core at C_1. It may, therefore, be emphasized that a proper identification of all of the critical points is crucial. Here, for instance, if $\theta_3^j > 0$, B is to be monitored against A, whereas for $\theta_3^j < 0$, the scene of interest shifts to C.

Method 3: Two-Plane Projection

This is simply an extension of the pair-of-tips method where graphical representation of motion of the entire system is attempted. Instead of one pair, we consider a triplet of points consisting of the center of mass of the core, the nose of the strap-on, and the bottom center of the strap-on under consideration. The relative motion of both the nose as well as the bottom center of the strap-on is examined with reference to the center of mass of the core. The analysis of projection of these two relative position vectors on two appropriate planes is the essence of this method. These are usually the radial and the transverse planes. To facilitate animation of the relative motion of a falling strap-on, we depict it by a straight line that connects its nose with its bottom center. Such a representation of the strap-on naturally demands an all-round enlargement in the size of the parent body by an amount equal to the strap-on radius. This leads to a somewhat conservative assessment, however. To demonstrate the power of the method, a complex collision situation is considered as shown in Fig. 4 where out of the six strap-ons only two, namely, strap-ons 1 and 3, are separating. Here, presence of the nonseparating strap-ons complicates the situation considerably. Figure 4 shows the sequence of moving projections of the centerlines of the strap-ons 1 and 3 in the radial as well as the lateral planes during separation. The arrow is used to denote the nose of the strap-on in this figure. Needless to say, the projected strap-on centerline must hit at the enlarged boundary of the body (shown in dotted line) in both the views before the collision can occur.

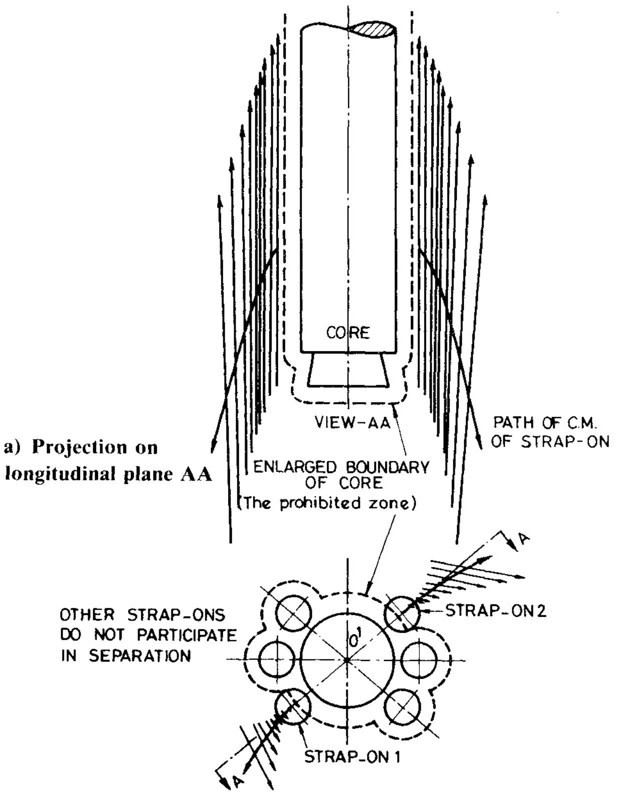

a) Projection on longitudinal plane AA

b) Projection on a lateral plane

Fig. 4 Projected line representation of the falling strap-ons.

It may be observed that these three methods have to be used suitably, alone or in combination, to enable identification of collisions, if any, in any general situation.

Attitude Motion of Core

In view of the nonideal control system, the actual attitude motion of the core generally differs from the prescribed one [Eqs. (3)]. We therefore focus our attention on the upper limits for attitude deviation of the core from its ideal behavior that can be tolerated without jeopardizing collision-free separation. It is possible to develop this useful information from an assumed nominal attitude motion of the core.

As before, we model the strap-ons as cylinders (Fig. 5). For a given position and orientation of the body j, the permissible angular excursion ζ can be determined as an angle by which the line O^1Q turns before coming in contact with the jth body at Q_1. A simple analysis of geometry of the separating bodies at the instant of possible collision enables us to obtain the following algebraic equations:

$$h^{*^2}\sec^2\theta_3^j + 2h^*\tan\theta_3^j(r_S^j - d^j/2\sec\theta_3^j - h_S^j\tan\theta_3^j) + [(r_S^j - d^j/2\sec\theta_3^j - h_S^j\tan\theta_3^j)^2 - (D^2/4 + l_0^{j^2})] = 0 \tag{20}$$

$$r^* = h^*\tan\theta_3^j + (r_S^j - d^j/2\sec\theta_3^j - h_S^j\tan\theta_3^j) \tag{21}$$

$$\zeta_0 = \arctan(D/2l_0^j) \tag{22}$$

$$\zeta = \arctan(r^*/|h^*|) - \zeta_0 \tag{23}$$

where (r^*, h^*) are the coordinates of the point Q_1 in the r-h plane, and of the two solutions for h^* available from Eq. (20), only the lower one is of consequence. If, however, Eq. (20) does not lead to a real solution or if $O^jQ_1 > \{d^{j^2}/4 + l^{j^2}\}^{1/2}$, an unlimited excursion would be permissible for the core.

Results and Discussion

The methodology developed here has been utilized in some of the ongoing in-house projects.[10-12] A few typical results are presented in the following.

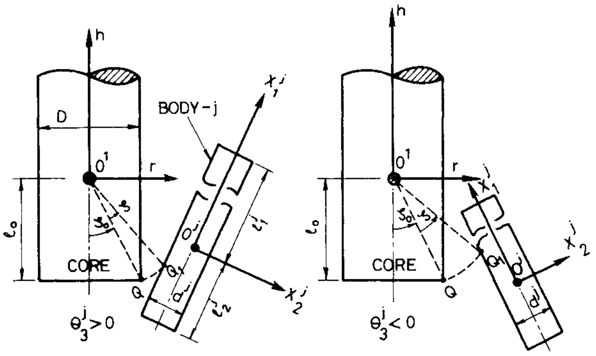

a) Geometry

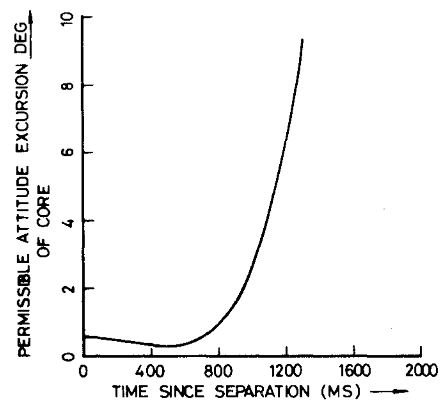

b) Permissible attitude excursion

Fig. 5 Geometry of separation with permissible core attitude excursion.

Example 1

Here, we consider the system with each strap-on having a pair of side thrusters. The relevant system parameters are given in Table 1. This investigation uses the three methods as described earlier to study each of the three different cases with thrust levels varied only for the lower thrusters. In view of symmetry of the strap-on configuration, it is sufficient to examine dynamics of only one of these.

Equation (18) is utilized to generate the no-collision zone (Fig. 2). It is evident that case 1 represents a collision-free separation, whereas in case 2, the positive angle (θ_3^j) buildup is too large for the lateral gap generated to cope up, and, hence, the bottom face of the strap-on ends up hitting the core. On the contrary, case 3 illustrates an example wherein the nose of the strap-on turns inward, leading to its collision with the core. Similar conclusions were reached from the simulation results based on methods 2 and 3 (Figs. 3, 4, and 6).

Example 2

In the second illustrative example, we use a black-box model for developing the no-collision zone in design parameter space. The dynamics again are planar, requiring only two basic parameters to be specified—the radial velocity Δv_2^j and

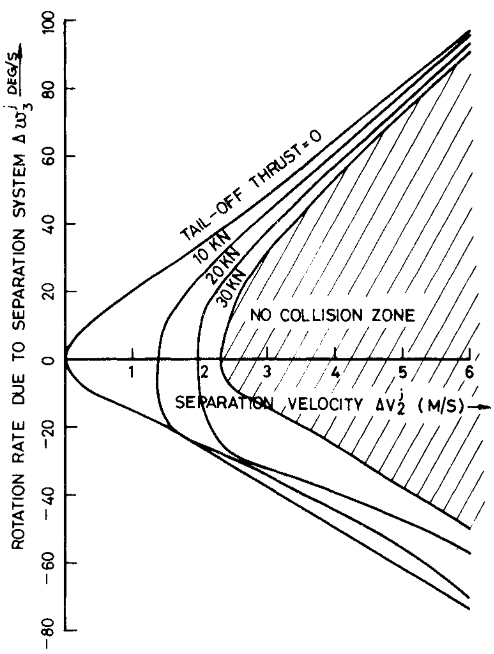

Fig. 7 Specification envelope for separation system.

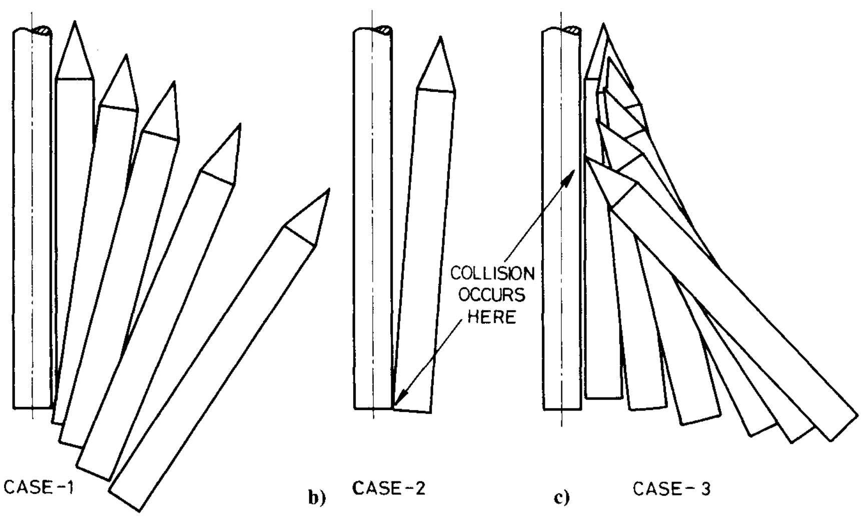

Fig. 6 Planar schematic representation of the falling strap-ons depicting possible modes of collision: a) case 1; b) case 2; c) case 3.

the rotational velocity $\Delta\omega_3^j$. The permissible zone is therefore constructed in terms of Δv_2^j and $\Delta\omega_3^j$ for several tail-off thrust levels (Fig. 7). It is normally difficult to predict the tailoff thrust a priori and only its upper bound may be available as a design input. Yet the requisite specification envelope can be obtained simply as the largest safety zone common to all such regions, which, therefore, dictates the design in such situations.

Conclusions

The basic equations of motion are developed for simulation of dynamics of the ongoing stage as well as the separating strap-ons. Geometry of collision in the multibody systems is analyzed. Three different methods, each with its own merits and demerits, are proposed for detection of collision. The methodology is illustrated using suitable examples. The simple black box model is found to be quite effective in constructing the no-collision zone in the parameter space for designing separating systems. Finally, the geometric analysis undertaken in this investigation enables us to determine the upper limits on the permissible core attitude excursions for safe separation—a rather important specification required to be imposed on the core control system.

References

[1]Dwork, M., "Coning Effects Caused by Separation of Spin Stabilized Stages," *AIAA Journal,* Vol. 1, No. 11, 1963, pp. 2639–2640.

[2]Wilke, R. O., "Comments on Coning Effects Caused by Separation of Spin Stabilized Stages," *AIAA Journal,* Vol. 2, No. 7, 1964, p. 1358.

[3]Longren, D. R., "Stage Separation Dynamics of Spin Stabilized Rockets," *Journal of Spacecraft and Rockets,* Vol. 7, No. 4, 1970, pp. 434–439.

[4]Waterfall, A. P., "A Theoretical Study of the Multispring Stage Separation System of the Black Arrow Satellite Launcher," Royal Aerospace Establishment, TR-682016, Farnborough Hants, UK, Aug. 1968.

[5]Subramanyam, J. D. A., "Separation Dynamics Analysis for a Multistage Rocket," *Proceedings of the International Symposium on Space Science and Technology,* edited by Shigeo Kobayashi, AGNE Publishing, Tokyo, 1973, pp. 383–390.

[6]Chubb, W., "The Collision Boundary Between the Two Separating Stages of the SA-4 Saturn Vehicles," NASA TN-D-598, Aug. 1961.

[7]Biswas, K. K., "Aspects of Non-Separating Apogee Motors," *Journal of Spacecraft and Rockets,* Vol. 21, No. 6, 1984, pp. 594–596.

[8]Lochan, R., Sasidharan, K. G., and Biswas, K. K., "A Study on Separation Dynamics of APPLE," Indian Space Research Organisation, ISR0-VSSC-TR-15-78, Bangalore, India, July 1978.

[9]Lochan, R., Sasidharan, K. G., and Biswas, K. K., "Eulerian Analysis of Multistep Separation Dynamics," *Proceedings of the 23rd Congress of ISTAM,* edited by J. S. Rao, Globe Printers, Allahabad, 1978, pp. 38–48.

[10]Prahlad, T. S., "A Profile of Aerodynamic Research in VSSC with Application to Satellite Launch Vehicles," *Sadhana,* Vol. 12, Pts. 1 and 2, Feb. 1988, pp. 125–182.

[11]Sundaramurthy, H., Narayan, K. Y., Suryanarayana, G. K., Lochan, R., Sasidharan Nair, K. G., and Varambally, B. S., "Wind Tunnel Investigation of Strap-On Booster Separation Characteristics of a Launch Vehicle," *Journal of Aeronautical Society of India,* Vol. 38, No. 4, 1986, pp. 215–221.

[12]Biswas, K. K., "Some Aspects of Jettisoning Dynamics Related to Launch Vehicles," *Space Dynamics & Celestial Mechanics,* edited by K. B. Bhatnagar, Reidel, Holland, 1986, pp. 369–379.